Journal of Rock Mechanics and Geotechnical Engineering. 2011, 3 (2): 153–160

Journal of Rock Mechanics and Geotechnical Engineering

Journal online: www.rockgeotech.org

A non-Archimedean number system to characterize the structurally inhomogeneous rock behavior nearby a tunnel

S. V. Lavrikov, O. A. Mikenina, A. F. Revuzhenko*

Institute of Mining, Siberian Branch, Russian Academy of Sciences, Novosibirsk, Russia

Received 15 February 2011; received in revised form 12 May 2011; accepted 1 June 2011

Abstract: The development of mathematical models of structurally inhomogeneous media leads to the necessity to consider structure of space itself where deformation occurs, i.e. change of mathematical apparatus itself. The space, whose coordinate axes are non-Archimedean straight lines, has been considered. Refusing the fulfillment of Archimedes's law allows to describe multi-scaling of the space, and so to consider deformation processes on different scale levels. The construction of two-scale mathematical model of rock masses has been considered as an example. The constitutive equations have been formulated on micro- and macro-levels and interaction condition between different levels as well. On micro-level, the elastic behavior of grains and plastic sliding between grains with possible softening are taken into account. On macro-level, the model represents a nonlinear system of equations describing the anisotropic rock mass behavior. On the basis of model, the numerical algorithm and code have been carried out to solve the plane boundary value problems. Examples of numerical simulations of stress-strain state of structural rock masses nearby a tunnel opening are presented. The deformation contours and isolines of stresses are plotted.

Key words: rock mass; inhomogeneity; mathematical model; non-Archimedean analysis; constitutive equations

1 Introduction

Actually, it is common to represent a rock mass as a medium composed of hierarchically structured levels as proposed by Sadovsky [1] based on some earlier studies, such as Revuzhenko et al. [2]. Mathematical modeling of rock behavior should anyhow consider the levels of internal structure amenable to a certain hierarchy. Modern mathematical models are generally built within the framework of the traditional continuum mechanics, and the description of the behavior of structural elements involves internal variables [3]. The same approach is applied to describing the deformation of metals [4]. However, development of the approach mentioned above suggests that a real variable itself should have an internal structure. This outcome calls for the necessity of changing one of the key conceptions in the traditional mathematical analysis, namely, the real straight line conception. It is worth saying that this issue emerges in the fields of plastic shaping of metals [5], theory of optimal control [6] as well as the theoretical mathematics (complimentary to rock mechanics), and many studies have devoted to it. The given study has been based on Refs.[7–10] and the considerations from Revuzhenko [11].

2 Model of a medium with an internal structure

To analyze an example of mathematical modeling of a rock mass taking into account two different scale levels, according to the principal idea proposed by Revuzhenko [11], we introduce an actual infinitely small quantity E, which is a positive number less than any number of the type of $\frac{1}{n}$, where n is an arbitrary positive whole number. In the case of plane deformation, we assume that

$$\left.\begin{aligned} X_1 &= x_1 + \xi_1 \\ X_2 &= x_2 + \xi_2 \end{aligned}\right\} \qquad (1)$$

where variables x_1, x_2, X_1 and X_2 are real numbers; $\xi_1 = y_1 E$; and $\xi_2 = y_2 E$. As a result, there appears "inward space" around each of the real numbers, i.e. a new scale level has been generated.

Doi: 10.3724/SP.J.1235.2011.00153
*Corresponding author. Tel: +7-3832170401;
E-mail: revuzhenko@yandex.ru
Supported by the Russian Foundation for Basic Research (10-05-91002) and the Integration Project of the Siberian Branch, Russian Academy of Sciences (69)

Let $\boldsymbol{u}$ be displacement vector. In the classical approach, $\boldsymbol{u}$ depends on two real variables. Derivatives of components of the vector determine the strain tensor and the turn. In this case, a displacement vector is related to four spatial coordinates (plane deformation as before):

$$\boldsymbol{u} = \boldsymbol{u}(x_1,\ x_2,\ \xi_1,\ \xi_2) \tag{2}$$

Derivatives with respect to ξ_1 and ξ_2 will govern the micro-strains, and derivatives with respect to x_1 and x_2 fix the macro-strains. We choose a simplest scenario in the possible set of mathematical models: transfering from micro-level to real level is possible to be described with the help of derivatives of functions. Deformations of a medium on a real-scale level and micro-levels are characterized with the following tensors:

$$\left.\begin{aligned} \varepsilon_{ij} &= \frac{1}{2}\left(\frac{\partial u_i}{\partial x_j} + \frac{\partial u_j}{\partial x_i}\right) \\ e_{ij} &= \frac{1}{2}\left(\frac{\partial u_i}{\partial \xi_j} + \frac{\partial u_j}{\partial \xi_i}\right) \end{aligned}\right\} \quad (i, j = 1,\ 2) \tag{3}$$

Their differences (together with residuation of turns) can describe the kinematics of processes at the interface of different scale levels.

The issue of stresses is more complex. It is possible to remove a part of complexity by replacing stresses by a function meant as the principal vector of internal forces: $\boldsymbol{f} = \{f_1, f_2\}$ [12]. Components of the vector $\boldsymbol{f}$ and the classical real scale stresses are related in terms of

$$\left.\begin{aligned} \sigma_{11} &= \frac{\partial f_1}{\partial x_2},\ \sigma_{12} = \frac{\partial f_2}{\partial x_2} \\ \sigma_{21} &= -\frac{\partial f_1}{\partial x_1},\ \sigma_{22} = -\frac{\partial f_2}{\partial x_1} \end{aligned}\right\} \tag{4}$$

Condition of twoness of shear stresses brings us an equation:

$$\mathrm{div}\boldsymbol{f} = \frac{\partial f_1}{\partial x_1} + \frac{\partial f_2}{\partial x_2} = 0 \tag{5}$$

So we know that the vector $\boldsymbol{f}$ may replace stress tensor in all the considerations. In that case, two equations of equilibrium relative to the stresses (given there are no mass forces) transfer to one of the relations in terms of Eq.(5), relative to the components of the vector $\boldsymbol{f}$. It is noted that formulae by Kolosov-Muskhelishvily include the function $\boldsymbol{f}$ as necessity. For elastic body, the parity of the vectors $\boldsymbol{u}$ and $\boldsymbol{f}$ is clear: in complex form, the formulae have equal structures relative to $u_1 + \mathrm{i}u_2$ and $f_1 + \mathrm{i}f_2$ [13].

Let us go back to the non-Archimedean plane (Eq.(1)): the function $\boldsymbol{f} = \{f_1, f_2\}$ is governed by the four variables, where f_1, f_2 can be described as

$$\left.\begin{aligned} f_1 &= f_1(x_1,\ x_2,\ \xi_1,\ \xi_2) \\ f_2 &= f_2(x_1,\ x_2,\ \xi_1,\ \xi_2) \end{aligned}\right\} \tag{6}$$

and its derivatives with respect to x_1 and x_2 are the real-scale level stresses (Eq.(4)) while its derivatives with respect to ξ_1 and ξ_2 are the micro-level stresses:

$$t_{11} = \frac{\partial f_1}{\partial \xi_2},\ t_{12} = \frac{\partial f_2}{\partial \xi_2},\ t_{21} = -\frac{\partial f_1}{\partial \xi_1},\ t_{22} = -\frac{\partial f_2}{\partial \xi_1} \tag{7}$$

Whatever, it follows that we have consistent conditions of stresses, which are rather difficult to be obtained in some other ways. Thus, we can get

$$\frac{\partial t_{11}}{\partial x_2} = \frac{\partial \sigma_{11}}{\partial \xi_2},\ \frac{\partial t_{12}}{\partial x_2} = \frac{\partial \sigma_{12}}{\partial \xi_2},\ \frac{\partial t_{21}}{\partial x_1} = \frac{\partial \sigma_{21}}{\partial \xi_1},\ \frac{\partial t_{22}}{\partial x_1} = \frac{\partial \sigma_{22}}{\partial \xi_1} \tag{8}$$

Now, formulation of constitutive equations included in the model needs experimental data, hypotheses about deformation mechanism, etc.. Therefore, we conduct our analysis based on an elastoplastic model of rocks [14]. According to Ref.[14], we assume that the medium on micro-level possesses grain structure, the pore space between grains is unfilled (pore material is absent), and there are relative slips over contact areas of grains. Let the effective grain package be located along coordinate axes, as shown in Fig.1, we have already mentioned above that in the non-Archimedean plane (Eq.(1)), derivatives of the displacement vector $\boldsymbol{u}$ components with respect to x_1 and x_2 fit averaged strains at the central points of particles; derivatives with respect to ξ_1 and ξ_2 fit the strains of the particles (micro-strains). Differences of the derivatives characterize slips over the contact surfaces of the particles.

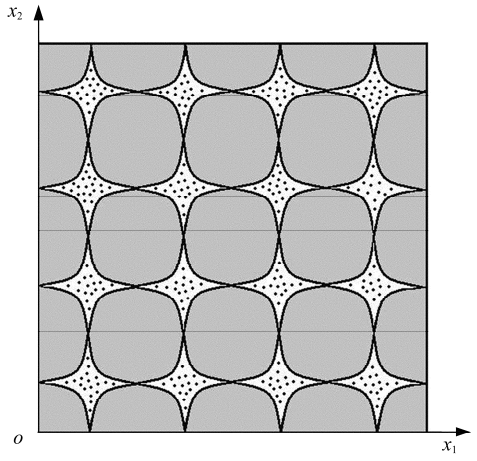

Fig.1 Effective grain package located along coordinate axes.

Let us discuss the structure of the constitutive equations. Absence of the pore material drives us at

$$t_{ij} = \sigma_{ij} \tag{9a}$$

or

$$\frac{\partial f_i}{\partial \xi_j} = \frac{\partial f_i}{\partial x_j} \quad (i,\ j = 1,\ 2) \tag{9b}$$

It seems inane to account for inhomogeneity of stresses and strains within the bounds of individual particles. Revuzhenko [14] used averaged characteristics of particles and assumed that they behaved elastically. In this case, considering Eqs.(4) and (9), the elastic behavior of grains (the Hooke's law for the plane deformation) can be described in the following form:

$$\left.\begin{aligned} \frac{\partial u_1}{\partial \xi_1} &= e_{11} = \frac{1-\nu}{2\mu}\frac{\partial f_1(x_1,\ x_2,\ 0,\ 0)}{\partial \xi_2} + \frac{\nu}{2\mu}\frac{\partial f_2}{\partial \xi_1} \\ \frac{\partial u_2}{\partial \xi_2} &= e_{22} = -\frac{1-\nu}{2\mu}\frac{\partial f_2}{\partial \xi_1} - \frac{\nu}{2\mu}\frac{\partial f_1}{\partial \xi_2} \\ \frac{\partial u_1}{\partial \xi_2} + \frac{\partial u_2}{\partial \xi_1} &= 2e_{12} = \frac{1}{\mu}\frac{\partial f_2}{\partial x_2} \end{aligned}\right\} \tag{10}$$

where ν and μ are the elastic constants.

Considering equations of transferring from a scale level to another scale level, following Ref.[14], we assume that at the interface of the scale levels (for slips between grains), the following equations hold true:

$$\left.\begin{aligned} \frac{\partial u_1(x_1,\ x_2,\ 0,\ 0)}{\partial x_1} &= \frac{\partial u_1(x_1,\ x_2,\ 0,\ 0)}{\partial \xi_1} \\ \frac{\partial u_2}{\partial x_2} &= \frac{\partial u_2}{\partial \xi_2} \\ \frac{\partial u_2}{\partial x_1} - \frac{\partial u_2}{\partial \xi_1} &= \frac{1}{G_1}\frac{\partial f_1(x_1,\ x_2,\ 0,\ 0)}{\partial x_1} \\ \frac{\partial u_1}{\partial x_2} - \frac{\partial u_1}{\partial \xi_2} &= \frac{1}{G_2}\frac{\partial f_1}{\partial x_1} \end{aligned}\right\} \tag{11}$$

where G_1 and G_2 are pre-set plastic moduli. The first two equations reflect the absence of dilatation (although it is of no difficulty to take dilatation into account), and the other two equations describe independent slips over the interface between two different families (see Fig.2).

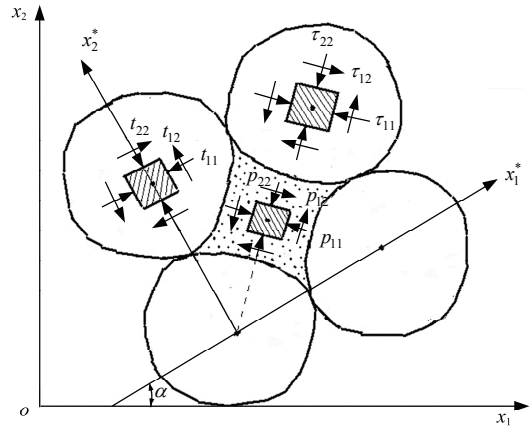

Fig.2 Structures of the medium on the micro-scale level.

Thus, we have obtained a set of equations (Eqs.(4), (9), (10) and (11)), i.e. twelve equations related to the four unknown functions f_i and u_i $(i = 1,\ 2)$ in total. The given set of equations is not over-determined as each of the functions depends on four (not two) arguments: $f_i = f_i(x_1,\ x_2,\ \xi_1,\ \xi_2)$ and $u_i = u_i(x_1,\ x_2,\ \xi_1,\ \xi_2)$. The nature of "complimentary" equation has close relations with the new spatial variables that emerge in the non-Archimedean space.

In order to find slipping conditions between grains (the second couple of Eq.(11)), we assume these conditions as nonlinear relationships of the shear stresses t_{ij} and slips $\gamma_i = \frac{\partial u_j}{\partial x_i} - \frac{\partial u_j}{\partial \xi_i}$ $(i, j = 1,\ 2;\ i \neq j)$ over the grain contacts, here i is the number of contacts between two different families. The process of slipping has three phases: strengthening, softening and a residual strength stage. Slips over the contacts of different families are unrelated, i.e. generally $\gamma_1 \neq \gamma_2$. The characteristic diagram of the described conditions is shown in Fig.3. As the diagram in the figure is not linear, we rewrite the two final equations in Eq.(11) incrementally:

$$\left.\begin{aligned} \Delta t_{12} &= G_1\left(\frac{\partial \Delta u_2}{\partial x_1} - \frac{\partial \Delta u_2}{\partial \xi_1}\right) \\ \Delta t_{12} &= G_2\left(\frac{\partial \Delta u_1}{\partial x_2} - \frac{\partial \Delta u_1}{\partial \xi_2}\right) \end{aligned}\right\} \tag{12}$$

where plastic moduli G_i $(i = 1,\ 2)$ are found in terms of the pre-set constants γ_i^*, γ_i^{**}, G^{e} and G^{p} (refer to Fig.3) as follows:

$$G_i = \begin{cases} G^{\mathrm{e}} & (0 \le \gamma_i < \gamma_i^*) \\ -G^{\mathrm{p}} & (\gamma_i^* \le \gamma_i < \gamma_i^{**}) \\ 0 & (\gamma_i^{**} \le \gamma_i) \end{cases} \tag{13}$$

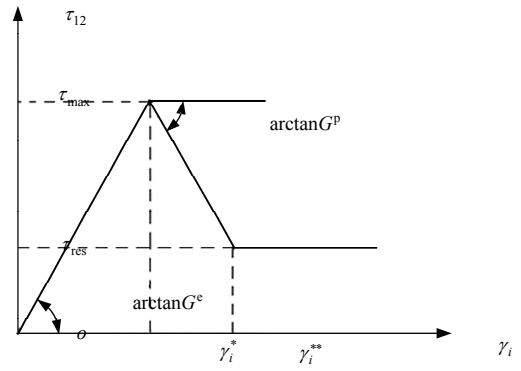

Fig.3 Diagram of sliding between grains on the micro-level.

So, it is here suggested that the medium softening occurs after the tangential stress reaches the maximum shear strength value $\tau_{\max}$ along sliding lines, connected with anisotropy directions (refer to Fig.3). In aforementioned model, this condition represents the failure criterion.

Thus, using the incremental form of Eq.(11) and the conditions of Eq.(9), the constitutive equations for the model at the macro-scale can be derived:

$$\left.\begin{aligned}
&\frac{\partial \Delta U_1}{\partial x_1}=\frac{1-\nu}{2\mu}\frac{\partial \Delta f_1}{\partial x_2}+\frac{\nu}{2\mu}\frac{\partial \Delta f_2}{\partial x_1}\\
&\frac{\partial \Delta U_2}{\partial x_2}=-\frac{1-\nu}{2\mu}\frac{\partial \Delta f_2}{\partial x_1}-\frac{\nu}{2\mu}\frac{\partial \Delta f_1}{\partial x_2}\\
&\frac{\partial \Delta U_1}{\partial x_2}+\frac{\partial \Delta U_2}{\partial x_1}=2\left(\frac{1}{2\mu}+\frac{1}{G_1}+\frac{1}{G_2}\right)\frac{\partial \Delta f_2}{\partial x_2}
\end{aligned}\right\} \tag{14}$$

Here, ΔU_i $(i=1,\ 2)$ means incremental components in terms of displacements in the centers of grains. So, the model can be written only in terms of macro-level parameters, i.e. the set of Eqs.(5) and (14) is a closed set applicable to the solution of boundary value problem. It is naturally required to analyze the micro-scale stress-strain state as the G_1 and G_2 in Eq.(14) are contingent on slips between the grains at micro-scale and they should be appropriately recalculated at every incremental step.

As it has been stated before, the coordinates of Eq.(14) are related to the effective regular package of grains, and the constitutive equations (Eq.(14)) are structured as ordinary equations of a linear-elastic body with coefficients ν^*, E^* and μ^*, where $\nu^*=\nu$, thus, we get

$$E^*=2\mu(1+\nu),\ \frac{1}{2\mu^*}=\frac{1}{2\mu}+\frac{1}{G_1}+\frac{1}{G_2} \tag{15}$$

where ν^*, E^* and μ^* may be regarded as the macro-Poisson's ratio, macro-Young's modulus and macro-shear modulus, respectively. However, unlike the classical elasticity, these coefficients are not mutually related, that is, $E^*\neq 2\mu^*(1+\nu^*)$, where ν^* and E^* are constants and governed by micro-parameters of grains; while μ^* is a stress function dependent on slips values over the contacts between grains, γ_i. Thus, this model can describe an anisotropic medium. It implies that the constitutive equations of the model have the form of Eq.(14) only in the coordinate system aligned with the effective package of grains. Formulation of the common closed set requires re-projecting the constitutive relations of Eq.(14) in an arbitrary coordinate system rotated at a random angle α (as a natural bedding angle) relative to the original coordinates and closing the system with the equilibrium equation (Eq.(5)). As a result, the closed incremental model is

$$\left.\begin{aligned}
&\frac{\partial \Delta f_1}{\partial x_1}+\frac{\partial \Delta f_2}{\partial x_2}=0\\
&\frac{\partial \Delta U_1}{\partial x_1}=A_{11}\frac{\partial \Delta f_1}{\partial x_2}-A_{12}\frac{\partial \Delta f_2}{\partial x_1}+A_{13}\frac{\partial \Delta f_2}{\partial x_2}\\
&\frac{\partial \Delta U_2}{\partial x_2}=A_{21}\frac{\partial \Delta f_1}{\partial x_2}-A_{22}\frac{\partial \Delta f_2}{\partial x_1}+A_{23}\frac{\partial \Delta f_2}{\partial x_2}\\
&\frac{\partial \Delta U_1}{\partial x_2}+\frac{\partial \Delta U_2}{\partial x_1}=A_{31}\frac{\partial \Delta f_1}{\partial x_2}-A_{32}\frac{\partial \Delta f_2}{\partial x_1}+A_{33}\frac{\partial \Delta f_2}{\partial x_2}
\end{aligned}\right\} \tag{16}$$

where Δf_1 and Δf_2 are the incremental internal force vectors; and the coefficient A_{ij} $(i, j = 1, 2, 3)$ depends on previous stresses and strains, micro-properties of grains and the anisotropy angle α (the lengthy coefficients are not presented here explicitly). The angle α is assumed to be known from the in-situ observations.

Thus, Eq.(16) represents the closed model to calculate increment in stresses and deformations at each step.

3 Problem formulation

The finite element algorithm and code have been developed based on the aforementioned model, allowing for computational investigation on plane stress-strain state in rocks. An extended tunnel with an arch cross-section in the zone $r\le R$, as shown in Fig.4, is chosen to study the rock deformation around it. The influence of rock mass weight is taken into account in the following way. Assuming that the horizontal overburden depth of the tunnel is H, some actual pressure σ_0 at this depth can be determined, for

instance, $\sigma_0 = -\gamma H$, where γ is the unit weight of rock. In real rock mass, the Coulomb's law is valid, i.e. $\tau_n = -\sigma_n \tan\varphi + c$, where φ is the actual friction angle, and c is the cohesion. Instead of the Coulomb's law, the law of plastic sliding shear is valid in the model above. It is characterized by two strength parameters: τ_{max} and τ_{res}. Therefore, the maximum shear strength (Fig.3) can be determined as $\tau_{max} = -\sigma_0 \tan\varphi + c$, i.e. some corrections are made to the plastic law taking into account the actual pressure at the tunnel depth [15]. Accordingly, the plastic shear law approximates the real tangential stresses at the depth H. The loading parameter is defined as a radial displacement V assigned at the outer boundary of the deformation zone ($r = R$). $V > 0$ is suitable for the direction toward the tunnel center. The inner bound of the tunnel is assumed stress-free. Sequently, the boundary conditions can be expressed as

$$\left.\begin{aligned} \Delta U_r\big|_{r=R} &= -V \quad (\Delta\sigma_n\big|_{\Gamma} = 0) \\ \Delta U_\theta\big|_{r=R} &= 0 \quad\;\; (\Delta\tau_n\big|_{\Gamma} = 0) \end{aligned}\right\} \qquad (17)$$

where ΔU_r and ΔU_θ are the components of incremental displacement vector in polar coordinates; $\Delta\sigma_n$ and $\Delta\tau_n$ are the normal and shear incremental stresses, respectively; and Γ is the inner bound of the deformation zone, whose geometry is defined with the pre-set constants a and b according to Fig.4.

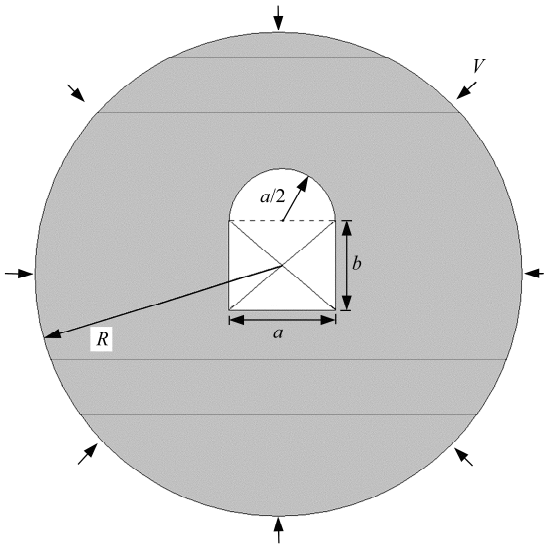

Fig.4 Problem formulation for the tunnel.

The well-formulated problem requires the initial conditions to be fixed and accord with the boundary conditions (Eq.(17)). The stresses, displacements and inter-grain slips at $t = 0$ can be written as

$$\sigma_{ij}^0 = 0, \qquad u_i^0 = 0, \qquad \gamma_i^0 = 0 \qquad (18)$$

where the superscript "0" specifies the iteration index.

Based on the known depth H and corresponding actual pressure σ_0, the correction to the maximum shear strength τ_{max} along sliding surfaces is determined. The increment of displacement on the external boundary leads to the increment of pressure. The loading procedure continues until the total pressure on the external boundary equals σ_0. As a result, the stress distribution in the rock mass is obtained when the pressure on the external boundary has the same order with σ_0, but the internal boundary is free from any stresses.

The closed model (Eq.(16)) with the boundary conditions (Eq.(17)) and initial conditions (Eq.(18)) allows the assessment of incremental stresses $\Delta\sigma_{ij}^n$ and incremental displacements ΔU_i^n at each loading step, where n is the iteration index (loading step). A global decision can be made as the iteration step increases: $\sigma_{ij}^{n+1} = \sigma_{ij}^n + \Delta\sigma_{ij}^n$, $U_i^{n+1} = U_i^n + \Delta U_i^n$, and $\gamma_i^{n+1} = \gamma_i^n + \Delta\gamma_i^n$.

As illustrated by the experience of problem solution with softening [16], stress will largely be governed by the value of softening modulus (slope of the descending part of the contact stress curve, G^p in Fig.3). Preliminary analysis of the model (Eq.(16)) makes and offers deduction on whether deformation process would be stable, or the elastic energy would be released beyond any control dynamically. We have to discuss different scenarios as it is possible that two families of inter-grain are asymmetrically active. For instance, the first contact stress curve is descending while the second one is ascending, namely, $\gamma_1^* < \gamma_1 < \gamma_1^{**}$ and $\gamma_2 < \gamma_2^*$, then the stable deformation takes place so long as it has

$$G_1^p < \frac{\mu G_2^e}{\mu + G_2^e} \qquad (19)$$

When the first contact stress curve is ascending and the second one is descending, we have the same relation with only subscripts "1" and "2" rearranged. When the both contact stress curves descend, the deformation is ensured to be stable if we have

$$\frac{G_1^p G_2^p}{G_1^p + G_2^p} < \mu \qquad (20)$$

Therefore, the descending curve (see Fig.3) must never exceed a certain threshold, or the stable process is violated.

4 Calculation results

The following parameters are adopted to conduct calculations: $R/b = 3.5$, $a/b = 1$, $\nu = 0.2$, $\mu = 2.5\times10^4$

MPa, $\gamma_1^* = \gamma_2^* = 0.001$, $\gamma_1^{**} = \gamma_2^{**} = 0.01$, $\alpha = 0°$, $\tan\varphi =$ 0.28, $c = 1.5$ MPa, $\tau_{res} = 2$ MPa, H = 500 m, and $\gamma = 25$ kN/m^3. According to these parameters, the actual pressure and the maximum shear strength can be calculated, i.e. $\sigma_0 = 12.5$ MPa and $\tau_{max} = 5$ MPa. In this case, the stability criteria are satisfied, and the deformation process will be stable.

The calculated deformation pattern is shown in Fig.5(a), where the white color shows the situation when the contact stress curve is ascending (strengthening phase), the grey color represents the descending curve (softening phase), and the black color indicates the areas matching the horizontal segment of the curve (residual strength stage). Incremental loading creates zones of softening and residual strength on the tunnel walls. First of all, four unrelated zones emerge in the directions of anisotropy of the rock masses. Further, loading supports the evolutions of these zones, one by one, at the depth from the tunnel walls toward surrounding rocks, while they are apt to coalesce on the tunnel surface (Fig.5(a)). Figures 5(b) and (c) show the isolines of deformation and the maximum shear stress at the beginning ($\tau = 0.5\sqrt{(\sigma_{11} - \sigma_{22})^2 + 4\sigma_{12}^2}$), respectively. The isolines of τ in Fig.5(b) illustrate the onset of deformation while the developed stress-strain state is depicted in Fig.5(c), which is in accord with the pattern in Fig.5(a). The shear stress τ reaches its maximal values at the corners of the tunnel contours (stress concentration happens at these corner points) and decreases with distance from the tunnel walls, inward surrounding rocks.

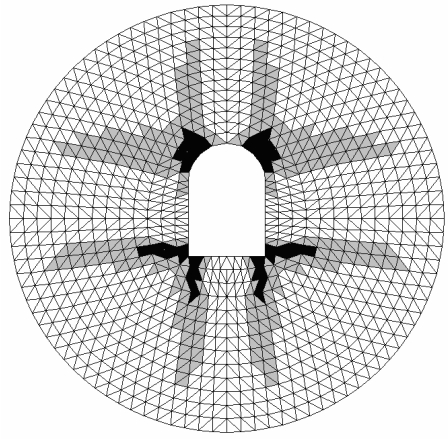

(a) Pattern of softening and residual strength zones.

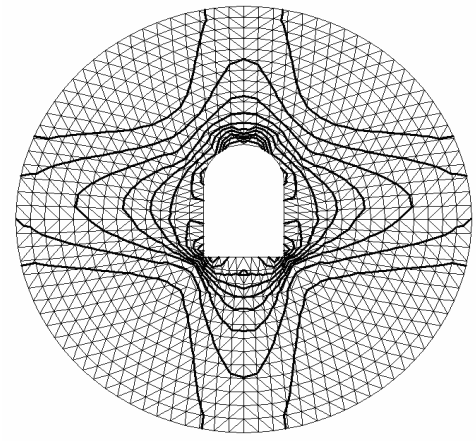

(b) Isolines of the maximum shear stress at the beginning.

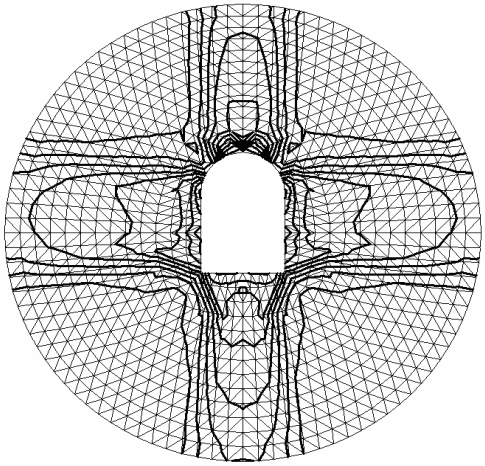

(c) Advanced isolines of the maximum shear stress.

Fig.5 Stable deformation with anisotropy $\alpha = 0°$.

To discuss another example, the same values of parameters as mentioned before are employed, except for γ_i^{**} at $\gamma_1^{**} = \gamma_2^{**} = 0.001\,2$ and for τ_{res} at $\tau_{res} = 0$ MPa, which will potentially break the stability equilibrium. According to calculations, deformation in this case is stable for a certain period of time, namely, until any contact achieves the descending part of the stress curve. Physically, uncontrolled dynamic energy release takes place in rocks at that time. However, this situation is not taken into account in the linear (incremental) calculation scheme, and further estimations bring a paradox result. It seems that after $G_i = -G^{\mathrm{p}}$ on any contact surface, $\Delta V > 0$ produces an opposite-direction slip over this contact: $\Delta\gamma_i < 0$. In other words, solution for $\Delta V > 0$ and any $\Delta\gamma_i > 0$ does not exist.

Lavrikov et al. [16] analyzed an artificial algorithm approach to step-by-step modeling of rock stresses with a post-limit softening modulus on inter-grain contacts, i.e. quasi-static formulation of the dynamic problem. Following Ref.[16], we impose a negative value to the increasing stress parameter: $\Delta V < 0$, and

find the solution in the following class: (1) on the contact surfaces where $G_i = -G^{\mathrm{p}}$, we assume $\Delta\gamma_i > 0$ (softening continues); and (2) on the contact surfaces where $G_i = G^{\mathrm{e}}$, $\Delta\gamma_i < 0$ (stress relief) is considered. At the contact surfaces where the material is not shear-resistant ($G_i = 0$) owing to $\tau_{\mathrm{res}} = 0$ MPa, the increasing $\Delta\gamma_i$ may have any sign (indifferent deformation). This kind of problem is resolvable, and the solution is unique and correct from the point of different modulus and stress relief. Solution with negative sign ($\Delta V < 0$) is built unless the softening contact arrives at the horizontal segment of the diagram. Physically, the negative value of load means an artificial displacement of equilibrium point on the softening segment of the diagram to another point on the horizontal segment, which exactly corresponds to the equilibrium situation after dynamical release of elastic energy. Then we assume again $\Delta V > 0$, and the process of loading continues. This calculated deformation mechanism is illustrated in Fig.6, and the grey areas of softening are absent herein.

If appearing, they immediately turn into the zones of shear strength loss (black areas in Fig.6). On the whole,

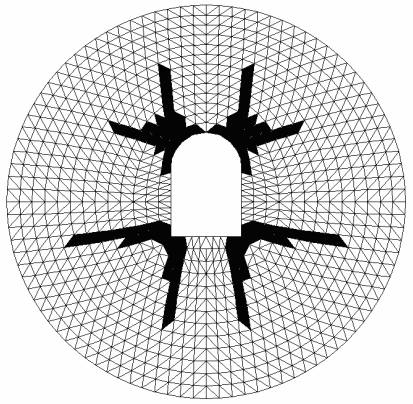

Fig.6 Zones of shear stress loss for unstable deformation with α = 0°.

geometries of these zones and persistent deformation are qualitatively alike.

It is illustrated that stress state at the onset is generally governed by the tunnel geometry, while later it is influenced greatly by the anisotropy of rocks: the areas of softening and residual strength expand at the bedding angle α toward axis Ox_1 and in orthogonal direction. In the calculations exemplified above, we select α = 0°, but the deformation patterns will be the same as that with α = 90° due to mutually orthogonal property of various families of contacts. In this context, an "opposite" situation will happen with α = 45°: the stable and unstable deformation patterns are presented in Figs.7(a) and 8, respectively. As for the isolines of τ, they will look like those in Fig.7(b) at the onset of

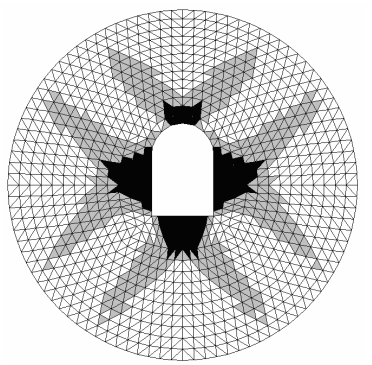

(a) Pattern of softening and residual strength zones.

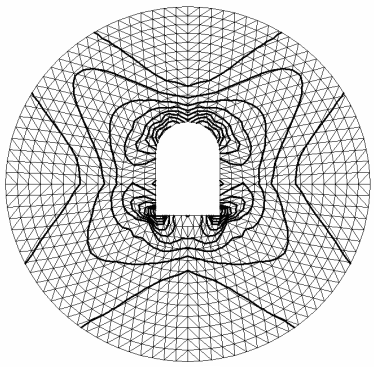

(b) Isolines of the maximum shear stress at the beginning.

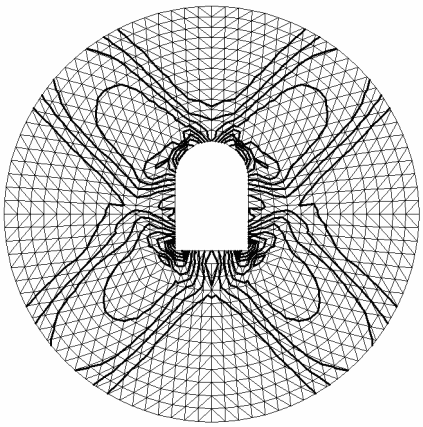

(c) Advanced isolines of the maximum shear stress.

Fig.7 Stable deformation with α = 45°.

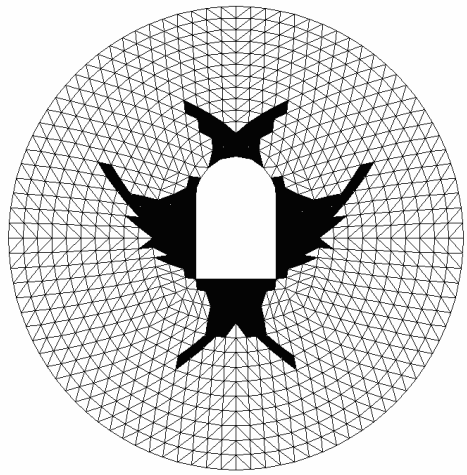

Fig.8 Zones of shear stress loss for unstable deformation with $\alpha =$ 45°.

the process. The pattern of deformation in Fig.7(a) corresponds to that of stress isolines in Fig.7(c).

5 Conclusions

(1) It is more suitable to apply an internal force vector instead of a stress tensor to the analysis of common properties of plane deformation models. In the equations relative to derivatives of the force vector (stresses) and derivatives of the displacement vector (strains), these vectors play a symmetric role.

(2) Sequential development of rock models carries the necessity to endow an independent variable and, thus, the space, with an internal structure.

(3) The authors have illustrated the process of constructing closed models of media with a hierarchy of structural levels by using non-Archimedean number system.

(4) The analysis involves the specific rock mass model, including two structural levels and takes account of anisotropy and softening on contact interfaces between elastic bearing grains.

(5) The proposed model was used as the basis to solve deformation of structurally inhomogeneous rocks around an extended tunnel. The patterns of deformation can illustrate the evolution of softening zones and areas of shear strength loss. It is shown that the geometry of the zone of material strength loss is greatly influenced by anisotropy directions in the model.

References

[1] Sadovsky M A. Natural lumpiness of rocks. Transactions of the Russian Academy of Sciences, 1979, 247 (4): 829–832 (in Russian).

[2] Revuzhenko A F, Stazhevsky S B, Shemyakin E I. Mechanism of deformation of a granular material under high shear. Journal of Mining Science, 1974, 10 (3): 374–377.

[3] Onami M, Iwasimidzu S, Genka K, et al. An introduction to micro-mechanics. Moscow: Metallurgia, 1987 (in Russian).

[4] Novozhilov V V, Kadashevich Y I. Micro-stresses in engineering materials. Leningrad: Machine-building, 1990 (in Russian).

[5] Krotov V F, Brovman M Y. Extreme plastic deformations of metals. [S.l.]: The USSR Academy of Sciences, Mechanics and Machine Engineering, 1962: 148–153 (in Russian).

[6] Krotov V F, Bukreev V Z, Gurman V I. New methods of variational calculus in the flight dynamics. Moscow: Mashinostroenie, 1969 (in Russian).

[7] Albeverio S, Fenstad J E, Hoegh-Krohn R, et al. Nonstandard methods in stochastic analysis and mathematical physics. London: Academic

Press, 1986.

[8] Davis M. Applied nonstandard analysis. New York: John Wiley and Sons, Inc., 1977.

[9] Klein F. Elementary mathematics from an advanced standpoint: geometry. New York: Macmillan, 1939.

[10] Uspensky V A. What is nonstandard analysis? Moscow: Nauka, 1987 (in Russian).

[11] Revuzhenko A F. Non-Archimedean space as the basis for or the mathematical body of geomechanics. In: Collected Works Devoted to the Shemyakin's 75th Anniversary. Moscow: Fizmatlit, 2006: 606–626 (in Russian).

[12] Lavrikov S V, Mikenina O A, Revuzhenko A F. Internal force vector and the non-Archimedean analysis approach to description of plane deformation of inelastic bodies. [S.l.]: [s.n.], 2009: 160–171 (in Russian).

[13] Muskhelishvili N I. Some basic problems of the mathematical theory of elasticity. 5th ed. Moscow: Nauka, 1966 (in Russian).

[14] Revuzhenko A F. Mechanics of elastoplastic bodies and the nonstandard analysis. Novosibirsk: Novosibirsk State University, 2000 (in Russian).

[15] Eremenko A A, Eremenko V A, Gaidin A P. Rock-geological and geomechanical conditions of iron-ore excavation in Altai-Sayan plicated region. Novosibirsk: Nauka, 2009 (in Russian).

[16] Lavrikov S V, Mikenina O A, Revuzhenko A F, et al. The concept of non-Archimedean multiscale space and models of plastic media with structure. Physical Mesomechanics, 2008, 11 (3): 233–246.